

## A NUMERICAL STUDY OF THE SIZE EFFECTS ON THE CRACK GROWTH RESISTANCE

G. X. Shan \*, O. Kolednik † and F. D. Fischer ‡

The size effects on the  $J_R$ -curve and the dissipation rate  $D$  are investigated numerically for a mild steel on CT specimens of three different sizes,  $W = 50, 200$  and  $800$  mm, and ligament to width ratios,  $b/W = 0.3, 0.46$  and  $0.6$ . The fracture process is controlled by the experimentally determined critical crack tip opening displacement  $CTOD_i$  for crack growth initiation and the critical crack tip opening angle  $CTOA_C$  for stable crack growth. The results show that for the investigated mild steel under plane strain conditions the  $J_R$ -curve depends only slightly on the specimen size whereas the dissipation rate  $D$  is a complicated function of the size.

INTRODUCTION

In recent years there has been considerable interest in the size effects on the elastic-plastic parameters for crack growth resistance of ductile materials. A large number of experimental investigations has been performed (see e.g. Braga and Turner (1), McCabe et al (2), Link et al (3), John and Turner (4), Etemad and Turner (5), Jones et al (6) and Schwalbe (7)). The aim is to examine whether the parameters measured on small laboratory test specimens can be transferred to real structures.

Since the  $J_R$ -curve can be easily determined from laboratory test specimens, it has been widely used as a measure of the crack growth resistance of ductile materials. However, more and more experimental results reveal that the  $J_R$ -curve is geometry dependent. Especially, the constraint which varies with the specimen geometries has a strong effect on the measured  $J_R$ -curve. The application of the  $J_R$ -curve for real

---

\*Christian-Doppler-Laboratorium für Mikromechanik der Werkstoffe, A-8700 Leoben, Austria.

†Erich-Schmid-Institut für Festkörperphysik der Österreichischen Akademie der Wissenschaften, A-8700 Leoben, Austria.

‡Institut für Mechanik, Montanuniversität Leoben, and Christian-Doppler-Laboratorium für Mikromechanik der Werkstoffe, A-8700 Leoben, Austria.

structures is still questionable.

As an alternative Turner (8) (9) introduced the dissipation rate  $D$  as a measure of the crack growth resistance.  $D$  has the similar feature to the  $J$ -integral that it can be easily determined experimentally. In Turner and Kolednik (10) and Kolednik (11) it was pointed out that  $D$ , compared to the  $J_R$ -curve, is a physically more reasonable measure of the crack growth resistance. The geometry dependence of  $D$  has not yet been investigated systematically.

In this paper stable crack growth in CT-specimens of three different sizes (specimen width  $W = 50, 200$  and  $800$  mm) of a mild steel is analysed with the elastic-plastic finite element method. Three different ligament to width ratios,  $b/W = 0.3, 0.46$  and  $0.6$ , are considered. The size effects on both the  $J_R$ -curve and the dissipation rate  $D$  are analysed.

### EXPERIMENTS

For the current investigation the already existing data of a  $J_{IC}$ -multi specimen test (Kolednik and Stüwe (12)) were used. The tests were conducted on CT-specimens having the following dimensions: width  $W = 50$  mm, thickness  $B = 25$  mm and original crack length  $a_0 \approx 27$  mm. The material is an annealed structural steel. The material properties are: elastic modulus  $E = 200$  GPa, yield stress  $\sigma_0 = 298$  MPa and ultimate tensile stress  $\sigma_u = 426$  MPa.

In (11) it was worked out clearly that in the regime of large scale yielding two parameters are needed to describe a fracture process: the crack growth initiation (or fracture initiation) toughness and the crack growth toughness. In our case the critical crack tip opening displacement,  $CTOD_i$ , for the crack growth initiation and the critical crack tip opening angle,  $CTOA_C$ , for the stable crack growth were applied as the input data for the numerical simulation of the fracture process. The  $CTOD_i$  values were measured by means of the stereophotogrammetry with a scanning electron microscope (Kolednik and Stüwe (13)). The  $CTOA_C$  values were determined from metallographical sections of the broken specimens (Shan et al (14)). Since no experiments were made on specimens with  $W = 200$  mm and  $W = 800$  mm, the same  $CTOD_i$  and  $CTOA_C$  values are assumed also for these specimens. This assumption is justified by the works of Kolednik and Kutlesa (15) and Gibson et al (16) which show that for deeply notched bend type specimens  $CTOD_i$  and  $CTOA_C$  do not change significantly with the geometry variations.

### FINITE ELEMENT ANALYSES

The elastic-plastic finite element analyses were performed by using ABAQUS (Hibbitt et al (17)). Eight-node isoparametric elements were adopted. The loading process was controlled by prescribing the load-line displacement,  $v_{LL}$ . The crack growth was modeled by the node release technique without node shifting. To simulate an increment of crack growth the crack tip node and the mid-side node of the tip element

were released and the nodal forces on these nodes were then removed gradually at a constant  $v_{LL}$ . The smallest element size (i.e. the increment of crack growth) was 0.1 mm.

The fracture process was controlled as following. When  $CTOD$  at the original fatigue crack tip reaches the critical value ( $CTOD_i$ ), the first crack growth step is made. After this point the crack growth process is controlled by a constant  $CTOA_C$ . When  $CTOA$  at the current crack tip reaches  $CTOA_C$ , the crack grows by a step. After that the specimen is further loaded until  $CTOA$  again reaches  $CTOA_C$ . This process is repeated until the desired crack extension is reached.

The analyses were done for specimens of three different widths,  $W = 50, 200$  and  $800$  mm with  $b/W = 0.3, 0.46$  and  $0.6$ , respectively. In these analyses, the  $CTOD_i$  and  $CTOA_C$  values, the amount of the crack extension, the crack growth increment as well as the sizes of the elements in the crack growth region were kept constant for all specimens. A total crack extension of 3 mm was simulated.

## RESULTS AND DISCUSSION

Because of the limit on the length of the paper we present here only results from the plane strain analyses. No direct comparison between experiments and analyses is made in this paper since for the investigated material only small plain sided specimens with  $W = 50$  mm,  $a \approx 27$  mm and  $B = 25$  mm were tested. For this geometry detailed comparisons between the experimental and numerical results can be found in (14). It was shown that with the measured values of  $CTOD_i$  and  $CTOA_C$  from the center region of a plain sided specimen the plane strain analysis has well simulated the fracture behaviour in the center region of the tested specimens. For example, the measured curve of the load-line displacement vs. the crack extension in the center region of the specimen agrees well with the curve from the plane strain analysis. In (14) it was also shown that for the load vs. displacement curve and the  $J$ -integral vs. crack extension curve neither the plane strain analysis nor the plane stress analysis can yield satisfactory agreement with the measured results from plain sided specimens.

Fig.1 shows the load vs. displacement curves for the three different sizes with  $b/W = 0.46$ . The load and the load-line displacement are scaled by the plastic limit load  $P_L$  ( $P_L = Bb^2\sigma_0/(2W + a)$  ASTM (18)) and the specimen width  $W$ , respectively. The point of crack growth initiation is marked. For other ligament to width ratios the curves are similar. Clearly, the deformation behaviour in the specimens of the various sizes is very different. In the small specimen with  $W = 50$  mm, general yielding has been reached even at the beginning of the crack growth, whereas in the large specimen with  $W = 800$  mm, small scale yielding conditions prevail.

The  $J_R$ -curves, however, are not much affected by the large difference of the deformation conditions in the specimens (Fig.2). For all the three ligament to width ratios the slopes of the  $J_R$ -curves decrease only slightly with the increase of the

specimen size. (Again in Fig.2 only the  $J_R$ -curves for  $b/W = 0.46$  are plotted. For other ligament to width ratios the curves are very similar). The  $J$ -integral is calculated from the sum of the elastic part and the plastic part according to the ASTM Standard (18). According to the old version of ASTM E813 (ASTM (19)) the  $J$ -integral can also be evaluated from the work of the applied forces,  $A$ , which is equal to the sum of the elastic strain energy stored in the specimen,  $W_{el}$ , and the plastic deformation energy,  $W_{pl}$ , if the surface energy on the newly created crack surface is ignored. In Fig.3, the curves of  $A$ ,  $W_{el}$  and  $W_{pl}$  (scaled by the area of the ligament) are plotted against the crack extension. It is shown that the reduction of the plastic deformation energy per unit ligament area due to the increase of the specimen size is nearly completely compensated by the increase of the elastic energy in the specimen. The total work done by the external forces scaled by the ligament area remains almost unchanged when the specimen size increases. Since the  $J$ -integral is determined by the total work of the applied forces, it is relatively independent of whether the specimen is in contained yield (when the specimen is large) or in uncontained yield (when the specimen is small).

In Shan et al (20) it was shown that the increase of the specimen size may cause a change of the out-of-plane constraint in plain sided specimens. Especially in the case when the thickness  $B$  is smaller than the ligament length  $b$ , the specimen in contained yield (larger specimen) has a noticeably larger out-of-plane constraint than the specimen in uncontained yield (smaller specimen). Therefore, a “bigger-lower pattern” of the  $J_R$ -curves can be observed for these specimens when the size is increased.

The energy dissipation rate  $D$  is defined as

$$D \equiv \frac{1}{B} \frac{d}{da} (W_{pl} + \Gamma) = \frac{1}{B} \frac{d}{da} (A - W_{el}), \quad (1)$$

where  $\Gamma$  is the surface energy which is negligible for ductile fracture.  $D$  can be seen as the total irreversible energy which must be put into a pre-cracked body to produce an increment of crack extension  $da$  (10). For ductile fracture,  $D$  measures the change rate of the plastic deformation energy with the crack growth. As already pointed out in (8),  $D$  is geometry dependent. In Fig.4 to Fig.6, the variations of  $D$  with the crack growth for the three different sizes are shown. Here  $D$  was calculated from  $W_{pl}$  which was directly evaluated from the finite element model. From these figures we can distinguish three different variation patterns of  $D$ . Under general yielding conditions  $D$  has a slightly decreasing value which is a function of the ligament length  $b$  (the large  $D$  values at the beginning stage of the crack growth are values for the blunting of the crack tip). From small scale yielding to the point before which no plastic deformation occurs in the region of the back face of the specimen, i.e., the plastic deformation is restricted to a small region around the crack tip,  $D$  increases with the crack growth but is independent of the ligament length. In fact,  $D$  is also independent of the specimen size when the plastic deformation is restricted to the region around the crack tip. This point can be verified by comparing the  $D$ -curves

of  $W = 200$  mm and  $W = 800$  mm for  $b/W = 0.6$ . After the plastic deformation in the back face region  $D$  becomes a complicated function of  $b$  and increases by a larger rate with the crack growth. Clearly, if in the case of contained yield the “remote” plastic deformation is not considered in the calculation of  $D$ ,  $D$  may be a geometry-independent parameter for the crack growth resistance, at least for CT-specimens under the plane strain condition. This is, however, very difficult to realize in experiments.

For the investigated structural steel, the  $D$ -value under general yielding conditions is roughly proportional to the ligament length. More exactly,  $D/b$  decreases with the increase of  $b$  for a fixed size and it decreases also with the increase of the size for a fixed  $b/W$  ratio.

The  $D$ - $\Delta a$ -curves yield additional information on the physics of the fracture process which would not be available if only  $J$ - $\Delta a$ -curves were recorded. For the two limiting cases, engineering lefm and general yielding, it seems very possible to find out how  $D$  is influenced by the specimen geometry.

#### SUMMARY

In this paper the size effects on the  $J_R$ -curve and the dissipation rate  $D$  are investigated with the finite element method. Stable crack growth in CT specimens of a mild structural steel was simulated for three different sizes,  $W = 50, 200$  and  $800$  mm, and ligament to width ratios,  $b/W = 0.3, 0.46$  and  $0.6$ . The results can be summarized as following:

1. The  $J_R$ -curves depend only slightly on the specimen size although for the investigated three sizes the deformation state in the specimens is very different. This is because the  $J$ -integral is actually determined by the work of the applied forces scaled by the ligament area which, for a given crack extension, remains nearly constant when the size increases.
2. The dissipation rate  $D$  is a complicated function of the specimen size. On the first line, it depends on whether the specimen is in contained yield or uncontained yield. Only when the plastic deformation is restricted in the region around the crack tip  $D$  does not depend on the size and the ligament length.

These results may represent typical size effects of low-strength/high-toughness materials under plane strain conditions (approximately for side-grooved specimens). For this class of materials many experimental data in the literature showed no size effects on the  $J_R$ -curve. However, there are reported other size effects in the literature which are not included in this paper. They are related either to plane sided specimens with combined effects of the size and the thickness or to other material groups.

REFERENCES

- (1) Braga, L. and Turner, C. E., Fracture Mechanics: Twenty-Second Symposium (Volume I), ASTM STP 1131, Edited by H. A. Ernst, A. Saxena and D. L. McDowell, ASTM, Philadelphia, 1992, pp.178–197.
- (2) McCabe, D. E., Landes, J. D. and Ernst, H. A., Elastic-Plastic Fracture: Second Symposium, Volume II — Fracture Resistance Curves and Engineering Applications, ASTM STP 803, Edited by C. F. Shih and J. P. Gudas, ASTM, Philadelphia, 1983, pp.II-562–II-581.
- (3) Link, R. E., Landes, J. D., Herrera, R. and Zhou, Z., Defect Assessment in Components — Fundamentals and Applications, ESIS/EGF9, Edited by J. G. Blauel and K.-H. Schwalbe, Eds., Mechanical Engineering Publications, London, 1991, pp.707–721.
- (4) John, S. J. and Turner, C. E., Fat. & Fract. Engng Mats & Struct., Vol.13, 1990, pp.95–107.
- (5) Etemad, M. R. and Turner, C. E., J. Strain Anal., Vol.20, 1985, pp.201–208.
- (6) Jones, R. L., Gordon, J. R. and Challenger, N. V., Fat. & Fract. Engng Mats & Struct., Vol.14, 1991, pp.777–788.
- (7) Schwalbe, K.-H., Engng Fracture Mech., Vol.42, 1992, pp.211–219.
- (8) Turner, C. E., Fracture Behaviour and Design of Materials and Structures, Proceedings of ECF 8, Vol.II, EMAS U.K., 1990, pp.933–968.
- (9) Turner, C. E., Fracture Mechanics: Twenty-Second Symposium (Volume I), ASTM STP 1131, H. A. Ernst, A. Saxena, and D. L. McDowell, Eds., ASTM, Philadelphia, 1992, pp.71–92.
- (10) Kolednik, O. and Turner, C. E., 25. Vortragsveranstaltung des DVM-Arbeitskreises Bruchvorgänge, 1993.
- (11) Kolednik, O., Engng Fracture Mech., Vol.38, 1991, pp.403–412.
- (12) Kolednik, O. and Stüwe, H. P., Engng Fracture Mech. Vol.24, 1986, pp.277–290.
- (13) Kolednik, O. and Stüwe, H. P., Engng Fracture Mech., Vol.21, 1985, pp.145–155.
- (14) Shan, G. X., Kolednik, O., Fischer, F. D. and Stüwe, H. P., Engng Fracture Mech., Vol.45, 1993, pp.99–106.

- (15) Kolednik, O. and Kutlesa, P., Engng Fracture Mech., Vol.33, 1989, pp.215–223.
- (16) Gibson, G. P., Druce, S. G. and Turner, C. E., Int. J. Fracture, Vol.32, 1987, pp.219–240.
- (17) Hibbitt, H. D., Karlsson, B. I. and Sorensen, E. P., ABAQUS User's Manual Vers.5.2., 1993.
- (18) ASTM E813-87, Annual Book of ASTM-Standards, Section3, Vol.03.01, ASTM, Philadelphia, PA (1987).
- (19) ASTM E813-81, Annual Book of ASTM-Standards, Part10, ASTM, Philadelphia, PA (1981).
- (20) Shan, G. X., Kolednik, O. and Fischer, F. D., Constraint Effects in Fracture: Theory and Applications, ASTM STP 1244, Edited by M. Kirk and A. Bakker, ASTM, Philadelphia, 1994, to be published.

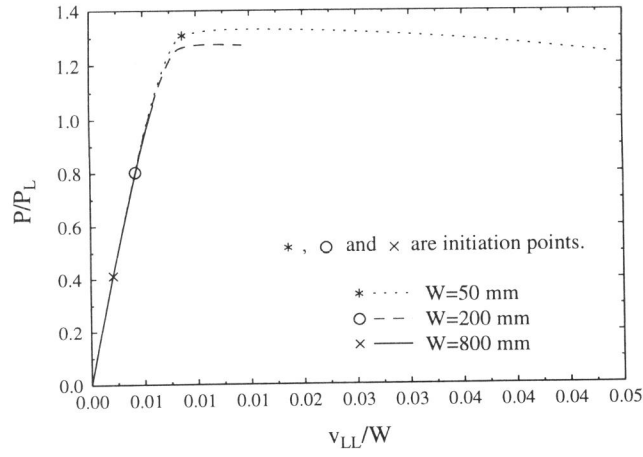


Figure 1: Load vs. displacement curves up to a crack extension of  $\Delta a = 3$  mm for three different sizes with  $b/W = 0.46$ , under plane strain conditions.

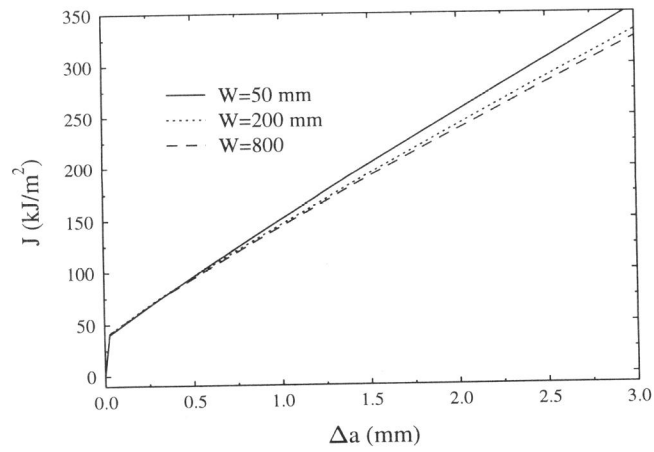


Figure 2:  $J_R$  curves for three different sizes with  $b/W = 0.46$ , under plane strain conditions.



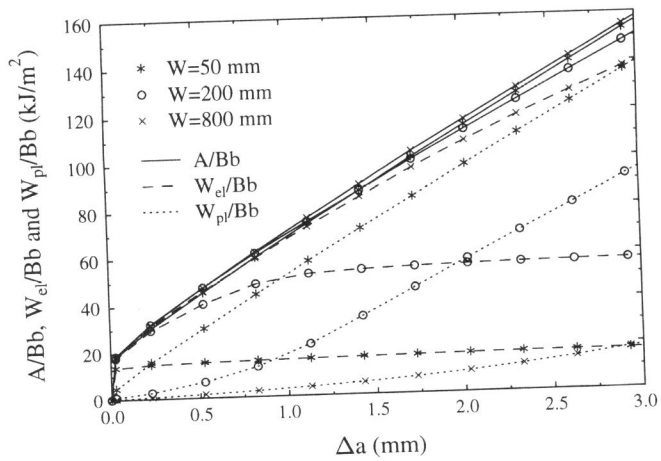


Figure 3: Variations of the work  $A$  of applied forces and the elastic and plastic deformation energy  $W_{el}$ ,  $W_{pl}$  with the crack growth in specimens of three different sizes with  $b/W = 0.46$ , under plane strain conditions.

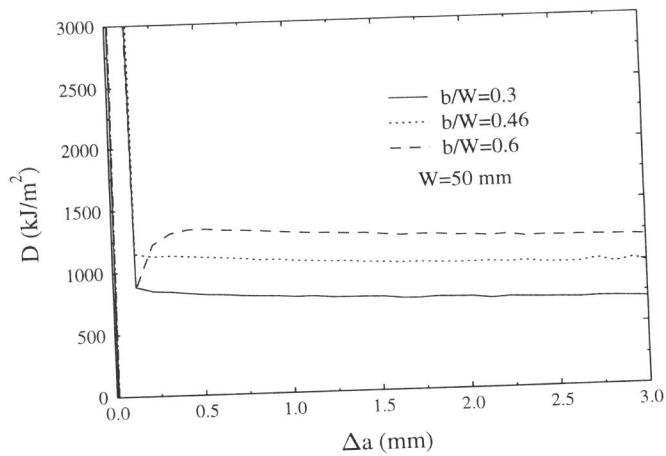


Figure 4: The variation of the dissipation rate  $D$  for three different ligament lengths  $b$  with  $W = 50$  mm, under plane strain conditions

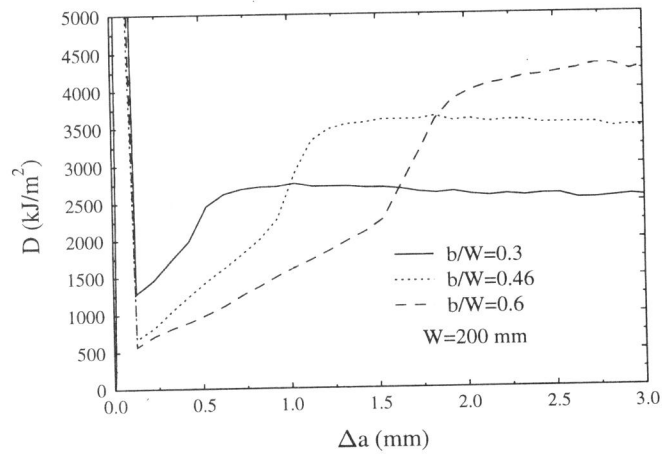


Figure 5: The variation of the dissipation rate  $D$  for three different ligament lengths  $b$  with  $W = 200$  mm, under plane strain conditions

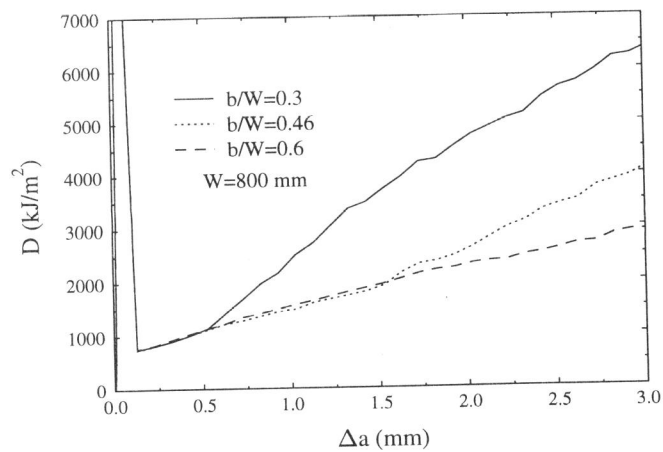


Figure 6: The variation of the dissipation rate  $D$  for three different ligament lengths  $b$  with  $W = 800$  mm, under plane strain conditions.